

# *Listeria monocytogenes* *aguA1*, but Not *aguA2*, Encodes a Functional Agmatine Deiminase

## BIOCHEMICAL CHARACTERIZATION OF ITS CATALYTIC PROPERTIES AND ROLES IN ACID TOLERANCE<sup>\*§</sup>

Received for publication, April 15, 2013, and in revised form, June 28, 2013. Published, JBC Papers in Press, August 5, 2013, DOI 10.1074/jbc.M113.477380

Changyong Cheng<sup>‡</sup>, Jianshun Chen<sup>§</sup>, Chun Fang<sup>‡</sup>, Ye Xia<sup>‡</sup>, Ying Shan<sup>‡</sup>, Yuan Liu<sup>‡</sup>, Guilan Wen<sup>‡</sup>, Houhui Song<sup>¶</sup>, and Weihuan Fang<sup>‡¶1</sup>

From the <sup>‡</sup>Zhejiang University Institute of Preventive Veterinary Medicine, Zhejiang Provincial Key Laboratory of Preventive Veterinary Medicine, and Key Laboratory of Molecular Animal Nutrition of the Ministry of Education, Hangzhou, Zhejiang 310058, China, the <sup>§</sup>Zhejiang Fisheries Technical Extension Center, Hangzhou, Zhejiang 310012, China, and the <sup>¶</sup>College of Animal Science and Technology, Zhejiang A&F University, Lin'an, Zhejiang 311300, China

**Background:** *Listeria monocytogenes* has two putative agmatine deiminase homologs, *AguA1* and *AguA2*.

**Results:** Only *AguA1*, but not *AguA2*, acts as functional agmatine deiminase and mediates acid tolerance in *L. monocytogenes*.

**Conclusion:** Provided is the first biological insight into the roles of AgDI in acid tolerance of *L. monocytogenes*.

**Significance:** We have discovered a novel residue Gly-157 other than the known catalytic triad (Cys-His-Glu/Asp) critical for *L. monocytogenes* AgDI activity.

*Listeria monocytogenes* is adaptable to low pH environments and therefore crosses the intestinal barrier to establish systemic infections. *L. monocytogenes* *aguA1* and *aguA2* encode putative agmatine deiminases (AgDIs) *AguA1* and *AguA2*. Transcription of *aguA1* and *aguA2* was significantly induced at pH 5.0. Deletion of *aguA1* significantly impaired its survival both in gastric fluid at pH 2.5 and in mouse stomach, whereas *aguA2* deletion did not show significant defect of survival in gastric fluid. With agmatine as the sole substrate, *AguA1* expressed in *Escherichia coli* was optimal at 25 °C and over a wide range of pH from 3.5 to 10.5. Recombinant *AguA2* showed no deiminase activity. Site-directed mutagenesis revealed that all nine *AguA1* mutants completely lost enzymatic activity. *AguA2* acquired AgDI activity only when Cys-157 was mutated to glycine. *AguA1* mutation at the same site, G157C, also inactivated the enzyme. Thus, we have discovered Gly-157 as a novel residue other than the known catalytic triad (Cys-His-Glu/Asp) in *L. monocytogenes* that is critical for enzyme activity. Of the two putative AgDIs, we conclude that only *AguA1* functionally participates in the AgDI pathway and mediates acid tolerance in *L. monocytogenes*.

*Listeria monocytogenes* is a Gram-positive food-borne pathogen that causes listeriosis with high mortality (1, 2). The bacterium is resistant to acidic environments where it encounters acidic food, such as processing environments, the stomach, and phagosomes of macrophages (3, 4). Agmatine deiminase (AgDI)<sup>2</sup> pathway is an acid tolerance mechanism described in

bacterial species like *Enterococcus faecalis* or *Streptococcus mutans* (5, 6). AgDI converts agmatine into putrescine and ammonia upon catalyzation (5, 7, 8). Agmatine enters bacterial cells via an agmatine-putrescine antiporter (*aguD*), where it is hydrolyzed to *N*-carbamoylputrescine by agmatine deiminase (EC 3.5.3.12) (9). Putrescine carbamoyltransferase (EC 2.1.3.6), encoded by *aguB*, mediates phosphorolysis of *N*-carbamoylputrescine, producing putrescine and carbamoylphosphate (10). Finally, a carbamate kinase (EC 2.7.2.2) transfers the phosphate group from carbamoylphosphate to ADP (Fig. 1A) (11). This pathway is thought to play an important role in acid resistance and competitive survival of *Lactobacillus brevis* (8).

AgDI is a member of the guanidinium-modifying enzyme family that hydrolyzes the guanidinium groups of agmatine, arginine, or methylarginine to form the ureido-containing derivatives (12). All enzymes of the guanidinium-modifying enzyme family contain a highly conserved catalytic triad (Cys-His-Glu/Asp), which plays a significant role in catalysis and substrate binding (12, 13).

The putative AgDI pathway in *L. monocytogenes* is encoded by the *agu* operon (14). There are two homologs, *AguA1* and *AguA2*, coded for by *aguA1* and *aguA2*, respectively (Fig. 1B). Sequence alignment of *L. monocytogenes* AgDI homologs to those from other species indicates that Asp-94, Glu-155, His-216, Asp-218, and Cys-356 might be the corresponding catalytic residues in both *AguA1* and *AguA2*. Listerial *AguA1* was initially annotated as a putative peptidyl-arginine deiminase (14). Homology analysis reveals that *AguA1* is actually an AgDI of the guanidinium-modifying enzyme family. Our previous study showed that this molecule was involved in acid tolerance because deletion of *aguA1* (*lmo0038* in strain EGD) led to reduced survival in acidic brain heart infusion broth at pH 4.0 (15).

This study further characterized the biochemical and catalytic properties of two AgDI homologs of *L. monocytogenes*, *AguA1* and *AguA2*, and their roles in acid stress response. We

\* This study was supported by National Natural Science Foundation of China Grants 31101829 and 31272570 and Natural Science Foundation of Zhejiang Province Grant Q12C190019.

§ This article contains supplemental Tables S1 and S2 and Fig. S1.

<sup>1</sup> To whom correspondence should be addressed: Inst. of Preventive Veterinary Medicine, Zhejiang University, 388 Yuhangtang Rd., Hangzhou, Zhejiang 310058, China. Tel. and Fax: 86-571-88982242; E-mail: whfang@zju.edu.cn.

<sup>2</sup> The abbreviations used are: AgDI, agmatine deiminase; ADI, arginine deiminase; BHI, brain-heart infusion; SOE, splice overlap extension.

## *L. monocytogenes* Agmatine Deiminase in Acid Tolerance

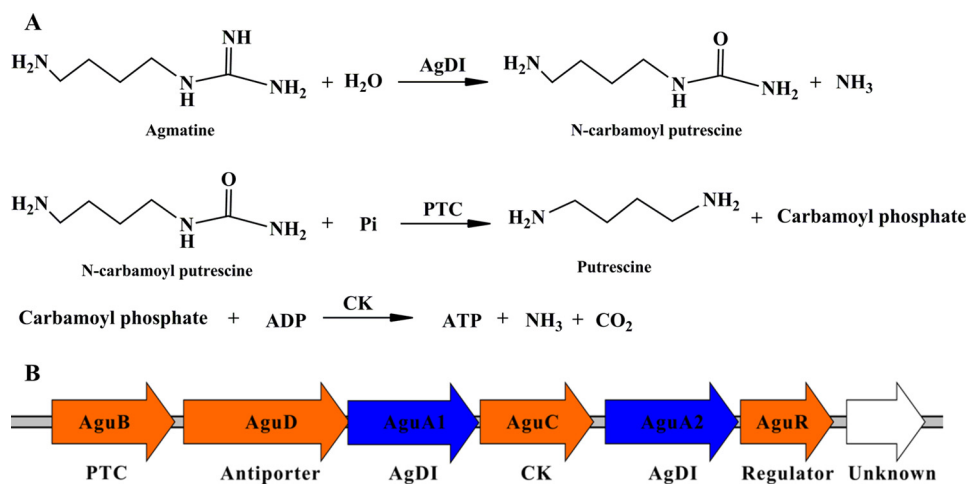


FIGURE 1. **The AgDI pathway and organization of the gene cluster in *L. monocytogenes*.** A, the AgDI pathway. Agmatine is first hydrolyzed to form *N*-carbamoylputrescine by AgDI. *N*-Carbamoylputrescine is then converted into putrescine and carbamoylphosphate by putrescine transcarbamoylase. Carbamate kinase (CK) then catalyzes the phosphate moiety in carbamoylphosphate to ADP, forming ATP as well as ammonia and CO<sub>2</sub>. B, genetic organization of the *L. monocytogenes* agmatine deiminase gene cluster.

conclude that *aguA1*, but not *aguA2* of *L. monocytogenes*, encodes a functional agmatine deiminase that contributes to acid tolerance, thus adding an additional acid stress response mechanism of *L. monocytogenes* other than the two well known glutamate decarboxylase and arginine deiminase (ADI) systems (10, 16–19).

### MATERIALS AND METHODS

**Chemicals**—Agmatine sulfate, *L*-arginine monohydrochloride, *L*-citrulline, diacetyl-monoxime, and thiosemicarbazid were purchased from Sigma-Aldrich. *N*-Carbamoyl-putrescine was synthesized by the Institute of Pesticide and Environmental Toxicology or Zhejiang University. All other chemicals of analytical reagent grade were obtained from commercial sources.

**Bacterial Strains, Plasmids, and Culture Conditions**—*L. monocytogenes* 10403S was used as the wild-type strain. *Escherichia coli* DH5 $\alpha$  was employed as the host strain for plasmids pMD18-T (Takara, Dalian, China), pET30a(+) (Merck), pERL3 (10) and pKSV7 (15, 20). *L. monocytogenes* was cultured in brain-heart infusion (BHI) medium (Oxoid, Hampshire, England). *E. coli* DH5 $\alpha$  and Rosetta (DE3) (Merck) were grown at 37 °C in LB broth (Oxoid). Stock solutions of ampicillin (50 mg/ml), erythromycin (50 mg/ml), kanamycin (50 mg/ml), and chloramphenicol (50 mg/ml) were added to the medium, where appropriate, at required levels.

**Bioinformatic Analysis**—The amino acid sequences of AguA1 and AguA2 of *L. monocytogenes* and its homologs in other microbial species were obtained from the National Centre for Biotechnology Information database. The sequences were aligned with Clustal X. Phylogenetic tree was constructed using the neighbor-joining method. The known crystal structure of *E. faecalis* agmatine deiminase (Protein Data Bank code 2JER) was acquired from the Protein Data Bank. Putative models of AguA1 and AguA2 were constructed using SWISS-MODEL Workspace (21–23).

**Transcriptional Analysis Using Quantitative PCR**—*L. monocytogenes* 10403S was grown to the stationary phase ( $A_{600} = 0.6$ ) in BHI broth at 37 °C and then exposed to acidic conditions

(pH 5.0) and neutral conditions (pH 7.0), respectively, for 60 min. Total RNA was extracted using the TRIzol method, and cDNA was synthesized with reverse transcriptase (TOYOBO, Osaka, Japan). Quantitative PCR was then performed in 20- $\mu$ l reaction mixtures containing SYBR quantitative PCR mix (TOYOBO) to measure transcriptional levels of *aguA1* and *aguA2* using an iCycler iQ5 real time PCR detection system (Bio-Rad) with specific primer pairs (supplemental Table S1). The housekeeping gene *gyrB* was used as an internal control for normalization as previously described (10). Relative transcription levels were quantified by the 2<sup>− $\Delta\Delta$ CT</sup> method and shown as relative fold changes in comparison with that at pH 7.0 (24). Transcriptional analysis was repeated for three times on each test condition.

**Construction of Deletion Mutants**—Genomic DNA of *L. monocytogenes* 10403S was extracted as described previously (25, 26). A homologous recombination strategy with SOE-PCR procedure was used for in-frame deletion to construct *aguA1* and *aguA2* single and double deletion mutants as described previously (15, 27). The DNA fragments containing homologous arms upstream and downstream of *aguA1* or *aguA2* were obtained by PCR amplification of 10403S DNA templates using the SOE primers (supplemental Table S1). Each of the SOE-PCR products with deletion of *aguA1* or *aguA2* was cloned into the temperature-sensitive shuttle vector pKSV7, which was then transformed into *E. coli* DH5 $\alpha$ . The recombinant vectors containing the target gene deletion cassettes were confirmed by sequencing. A previous protocol was followed for deletion of the targeted genes via allelic exchange (27). Briefly, the competent *L. monocytogenes* 10403S cells were electroporated with one of the vector constructs. Transformants were grown at a nonpermissive temperature (41 °C) in BHI medium containing chloramphenicol (10  $\mu$ g/ml) to promote chromosomal integration, and the homologous recombinants were passaged successively in BHI medium without antibiotic at a permissive temperature (30 °C) to enable plasmid excision and curing (28). The recombinants were identified as chloramphenicol-sensitive

## L. monocytogenes Agmatine Deiminase in Acid Tolerance

colonies and confirmed by PCR and DNA sequencing. The single deletion mutants  $\Delta$ aguA1 and  $\Delta$ aguA2 were generated initially. The mutant strain  $\Delta$ aguA1 was used in a second round of mutagenesis to construct the  $\Delta$ aguA1 $\Delta$ aguA2 double deletion mutants.

**Complementation of aguA1 Deletion**—To complement the *L. monocytogenes*  $\Delta$ aguA1 strain, the *aguA1* ORF with its promoter region was amplified from 10403S using primer pairs *aguA1-w/x* and *aguA1-y/z* by SOE-PCR (27) (supplemental Table S1). After restriction with appropriate enzymes, the PCR fragment was cloned into pERL3. The resulting plasmid was then electroporated into *L. monocytogenes*  $\Delta$ aguA1. The regenerated cells were plated on BHI agar containing erythromycin (5  $\mu$ g/ml). The complemented strain was designated as *L. monocytogenes*  $\Delta$ aguA1+aguA1.

**Survival in Synthetic Gastric Fluid**—Stationary phase cultures of *L. monocytogenes* 10403S, mutants ( $\Delta$ aguA1,  $\Delta$ aguA2, and  $\Delta$ aguA1 $\Delta$ aguA2), and complemented strain  $\Delta$ aguA1+aguA1 were harvested, washed in PBS, and resuspended in synthetic human gastric fluid (8.3 g/liter of proteose peptone, 3.5 g/liter of D-glucose, 2.05 g/liter of NaCl, 0.6 g/liter of  $\text{KH}_2\text{PO}_4$ , 0.11 g/liter of  $\text{CaCl}_2$ , 0.37 g/liter of KCl, 0.05 g/liter of bile, 0.1 g/liter of lysozyme, and 13.3 mg/liter of pepsin; adjusted to pH 2.5 with HCl) as described previously (16). After 30 min of incubation at 37 °C, the survival bacterial cells were plated onto BHI agar after appropriate dilutions. The plates were incubated at 37 °C for 24 h, and survival rates are reported as the means of three independent experiments, each performed in duplicate.

**Survival in Mouse Stomach**—ICR mice (20  $\pm$  2 g, female) were divided into five groups (eight mice per group) and acclimated for 3 days before experiments. Feed was removed 12 h prior to intragastric inoculation. Two-hundred  $\mu$ l of listerial cells containing 4–6  $\times$  10<sup>8</sup> CFU of wild-type, mutant, and complemented strains grown overnight in BHI medium at pH 7.0 was administered to mice of corresponding groups by intragastric inoculation using a ball-tipped gavage needle. At 1 h after inoculation, the stomach samples were separated and homogenized in sterile PBS (10 mM, pH 7.4). Serial dilutions of the homogenates were plated on PALCAM (*Listeria* selective medium) (Luqiao, Beijing, China) agar (29). The plates were incubated at 37 °C for 24 h for colony counting. A group of eight mice from the same batch was left uninoculated as controls that did not show visible colonies on PALCAM agar. The results were expressed as means  $\pm$  S.E. of log<sub>10</sub> CFU per stomach for each group. The animal experiments were approved by the Laboratory Animal Management Committee of Zhejiang University (approval no. 20111025).

**Prokaryotic Expression and Purification of AguA1 and AguA2**—AguA1 and AguA2 were expressed as fusion proteins to the N-terminal His tag using pET30a(+) as the expression vector. *E. coli* Rosetta (DE3) was used as the expression host. The full-length ORFs of *aguA1* and *aguA2* were amplified with primer pairs *aguA1-exp-F/R* and *aguA2-exp-F/R* (supplemental Table S1), respectively, and then inserted into the pET30a(+) vector after restriction digestion. The resulting plasmids were designated as pET-*aguA1* and pET-*aguA2*. *E. coli* cells harboring the recombinant plasmids were grown in 500 ml of LB medium supplemented with 50  $\mu$ g/ml kanamycin

at 37 °C until the cultures reached 0.6–0.8 at  $A_{600}$ . Isopropyl  $\beta$ -D-1-thiogalactopyranoside was then added to a final concentration of 0.4 mM to induce expression of AguA1 and AguA2 for 12 h at 15 °C.

The His-tagged fusion proteins AguA1 and AguA2 were purified using the nickel-chelated affinity column chromatography. Briefly, isopropyl  $\beta$ -D-1-thiogalactopyranoside-induced cell pellets were collected, resuspended in 50 mM PBS (pH 7.4), and disrupted with 100 cycles of sonication at 300 W for 5 s with intermittent cooling on ice for 10 s (25 min in total). After centrifugation at 12,000  $\times$  g for 20 min, the supernatant samples were collected and loaded onto a 2-ml prepacked nickel-chelated agarose gel column (Weishi-Bohui Chromtotech Co., Beijing, China). The columns were washed with PBS containing 500 mM NaCl and 30 mM imidazole, and the bound proteins were eluted with a linear gradient of 25–500 mM imidazole prepared in the same buffer. Expression and purification of recombinant proteins was analyzed by 12% SDS-PAGE followed by Coomassie Brilliant Blue staining. Protein concentration was quantified using the Bradford method for AgDI activity and kinetic assays. The purified enzyme AguA1 was stored in 50% glycerol at –80 °C.

**Site-directed Mutagenesis**—To identify the predicted active sites of AguA1 and AguA2, single site-directed mutants D94A, D94E, E155A, E155D, H216A, H216R, D218A, D218E, G157C, and C356A mutants for AguA1 and Y47E, C157G, F196L, N236D, and H360Q for AguA2 were generated on the vector template pET-*aguA1* or pET-*aguA2* using the QuikChange site-directed mutagenesis kit (Agilent, Santa Clara, CA) and the oligonucleotide primers (supplemental Table S2). The template DNA was removed by digestion with DpnI (TOYOBO) for 2 h at 37 °C. All mutants were sequenced to ensure that only the desired single mutations had been incorporated correctly into the wild-type expression constructs. The mutant proteins were expressed and purified as described above.

**Enzyme Kinetic Assays of AguA1 and AguA2**—The AgDI activity was assayed by monitoring production of ureido-containing compounds (30–33). Ureido groups (*i.e.*, citrulline and *N*-carbamoylputrescine) could react with diacetyl-monooxime under strong acidic conditions to generate a colorimetric chemical that absorbs at 530 nm. The coloring reagent consists of 1 volume of solution A and 3 volumes of solution B (solution A: 80 mM diacetyl-monooxime (Sigma) and 2.0 mM thiosemicarbazide (Sigma); and solution B: 3 M  $\text{H}_3\text{PO}_4$ , 6 M  $\text{H}_2\text{SO}_4$ , and 2 mM  $\text{NH}_4\text{Fe}(\text{SO}_4)_2$ ) (32). *N*-Carbamoylputrescine or citrulline formation was quantified from the calibration curves of reference chemicals at  $A_{530 \text{ nm}}$ .

The Michaelis-Menten kinetic curve was determined by incubating 2.5  $\mu$ M purified enzyme with varying amounts of agmatine (0–10 mM) in the assay buffer (100 mM potassium phosphate buffer, pH 7.5; final reaction volume, 500  $\mu$ l). The reaction was initiated by adding the enzyme and terminated by the addition of 100  $\mu$ l of 50% trichloroacetic acid (Sigma) after incubation at 25 °C for 30 min. Volumes of 120- $\mu$ l reaction samples were then mixed with 400  $\mu$ l of the coloring reagent. The mixtures were boiled at 100 °C for 5 min and then cooled down to room temperature for absorbance measurement at  $A_{530 \text{ nm}}$ . Product formation was quantified from the calibration



curves as described above. Enzymatic reaction rates ( $v_0$ ) versus substrate concentrations were fitted to a Michaelis-Menten equation (Equation 1) by a nonlinear regression method, and the values  $K_m$ ,  $V_{max}$ , and  $k_{cat}$  were determined by fitting the data to the equation using the program GraphPad Prism (GraphPad Software, San Diego, CA),

$$v_0 = V_{max}[S]/(K_m + [S]) \quad (\text{Eq. 1})$$

where  $[S]$  is the substrate concentration,  $v_0$  is the initial velocity,  $V_{max}$  is the maximum velocity, and  $K_m$  is the Michaelis-Menten constant for the substrate. The  $k_{cat}$  value was calculated from  $V_{max}$ , and the enzyme concentration  $[E]$  was calculated using the equation  $k_{cat} = V_{max}/[E]$ . One unit of enzyme activity corresponds to production of 1  $\mu\text{M}$  *N*-carbamoylputrescine  $\text{min}^{-1}$  or citrulline under the assay conditions.

**Metal Inhibition and  $IC_{50}$  Determination**—The effects of metal ions  $\text{Co}^{2+}$ ,  $\text{Cu}^{2+}$ ,  $\text{Fe}^{3+}$ ,  $\text{Mg}^{2+}$ ,  $\text{Zn}^{2+}$ , and  $\text{Ni}^{2+}$  on AguA1 activity were determined by preincubating the enzyme with varying concentrations (0–10 mM) of each metal ion for 30 min at 4 °C. The remaining procedures were the same as above. The 50% inhibitory concentration ( $IC_{50}$ ) is defined as the concentration of metal ions required for 50% decrease of maximum enzyme activity. The percentage of inhibition versus the logarithm of inhibitor concentrations was plotted, and the  $IC_{50}$  values were determined by using the program GraphPad Prism.

**Substrate Specificity and Competitive Assay**—To determine the substrate specificity of AguA1, arginine was used as another guanidinium-containing compound to test for its ability to act as the substrate or competitive binding inhibitor. The reaction was initiated by adding 10 mM agmatine and varying concentrations (0–10 mM) of arginine into the assay buffer (100 mM potassium phosphate buffer, pH 7.5; 500  $\mu\text{l}$  of final volume) containing 2.5  $\mu\text{M}$  enzyme. The remaining procedures were the same as above.

**Statistical Analysis**—All data comparisons were analyzed using the two-tailed homoscedastic Student's *t* test. In all cases, differences with *p* values of  $<0.05$  were considered as statistically significant. The GraphPad Prism 5 program was used for nonlinear fitting to the Michaelis-Menten equation.

## RESULTS

**Amino Acid Sequence Analysis of AguA1 and AguA2**—The two putative agmatine deiminases AguA1 and AguA2 of *L. monocytogenes* share a high level of amino acid sequence identity (67.7%) and are clustered together in the same branch. However, they form a sister branch to AgDIs from other species with 23.9–73.6% amino acid sequence identity (Fig. 2A).

Agmatine deiminases are members of the guanidinium-modifying family enzymes, a family that includes enzymes that hydrolyze the guanidinium groups of arginine, peptidyl-arginine, methylarginine, and agmatine to form the ureido-containing derivatives (12). A catalytic triad (Cys-His-Glu/Asp), which plays a significant role in substrate binding and catalytic activity, has been identified from the crystal structures of known ADIs (34–36). Although AgDIs show homology to ADIs with similar structures and reaction mechanisms, they differ in their substrates (5, 8, 30). Alignment with AgDIs from other

species indicates that Asp-94, Glu-155, His-216, Asp-218, and Cys-356 are the corresponding catalytic residues of *L. monocytogenes* AguA1 and AguA2 (Fig. 2B). However, there are five specific residues (Tyr-47, Cys-157, Phe-196, Asn-236, and His-360) of AguA2 differing from other AgDIs including AguA1, which might affect its agmatine deiminase activity (Fig. 2B). We modeled the structures of AguA1 and AguA2 using the crystal structure of *E. faecalis* AgDI (Protein Data Bank code 2JER) as the template (supplemental Fig. S1) (5). The predicted protein structures of AguA1 and AguA2 show high similarity to *E. faecalis* AgDI (supplemental Fig. S1), including a fanlike structure with five blades that result from a 5-fold pseudosymmetric structure in which each repeating element consists of a three-stranded mixed  $\beta$  sheet and a helix in a  $\beta\beta\alpha\beta$  arrangement (5, 30). These results suggest that AguA1 and AguA2 of *L. monocytogenes* are typical AgDIs that might exhibit agmatine deiminase activity.

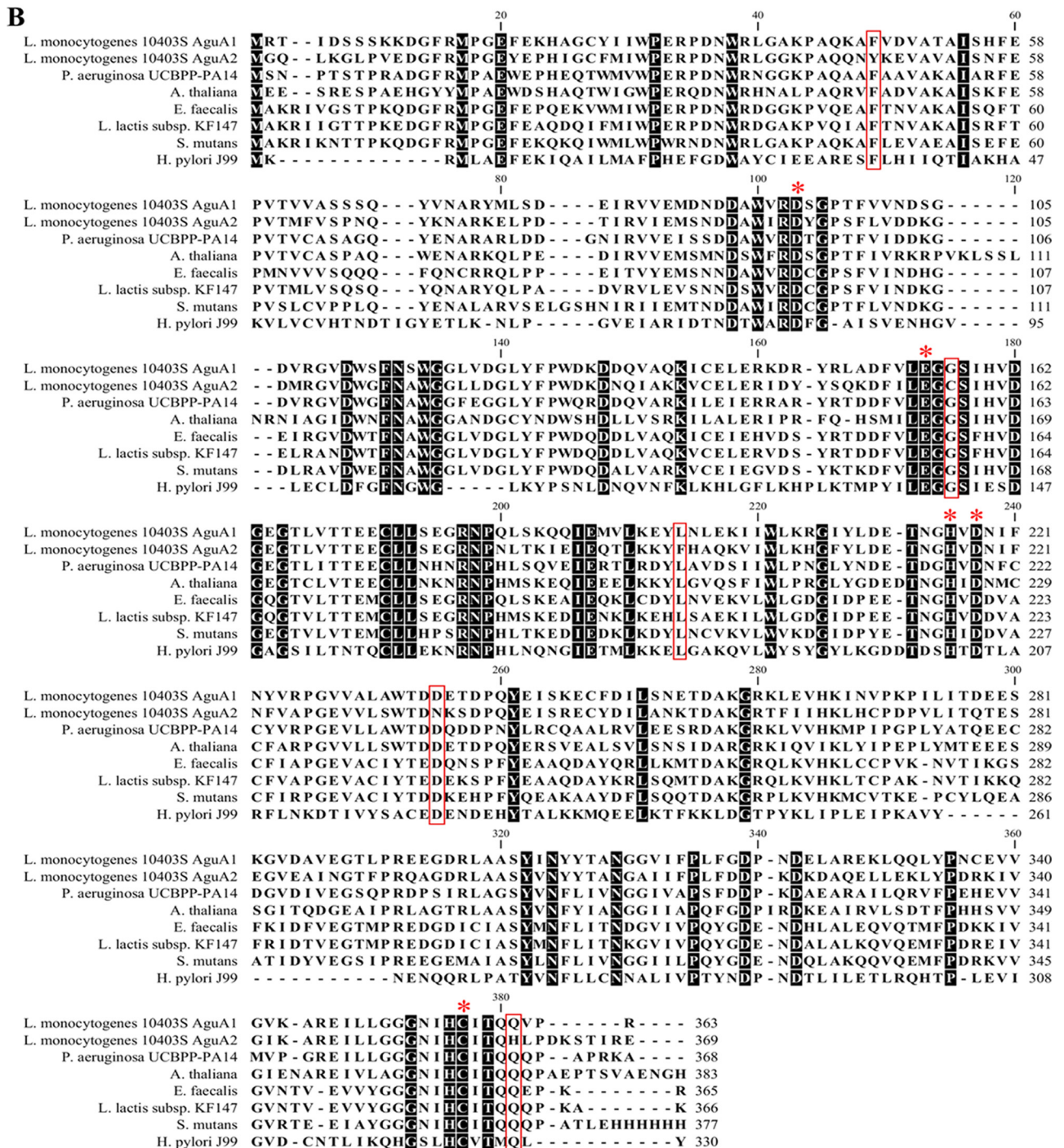
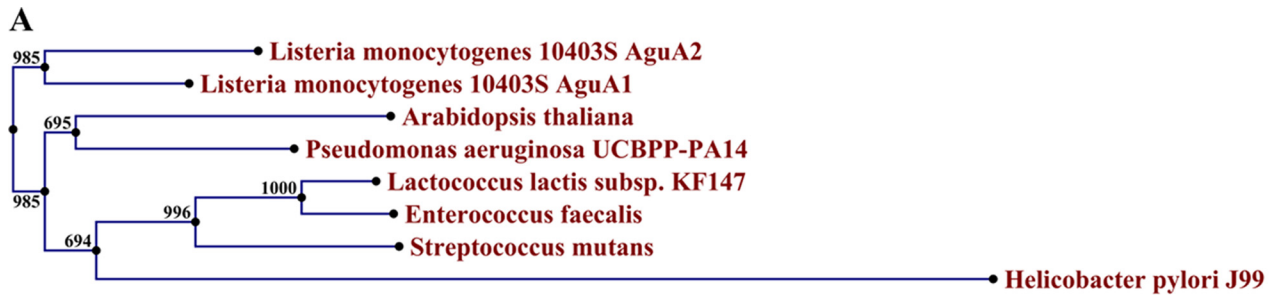
**AguA1, but Not AguA2, Mediates Acid Tolerance of *L. monocytogenes***—To investigate whether *aguA1* and *aguA2* were induced under acidic conditions, quantitative RT-PCR was conducted to assess relative gene transcription levels in response to acidic stress at pH 5.0. Transcription of both *aguA1* and *aguA2* was about 13- and 15-fold, higher at acidic pH 5.0 than at pH 7.0 with the statistical *p* values of 0.018 and 0.016, respectively (Fig. 3A).

To further determine whether *aguA1* and *aguA2* contribute to survival in acidic environments, *L. monocytogenes* 10403S, *aguA1/aguA2* single and double mutants and *aguA1* complement strain were exposed to synthetic gastric fluid at pH 2.5. Only the mutants  $\Delta\text{aguA1}$  and  $\Delta\text{aguA1}\Delta\text{aguA2}$  exhibited significant reduction in the survival rate as compared with the parent and complemented strains ( $p < 0.01$ ). Deletion of *aguA2* did not significantly impair its survival (Fig. 3B). Furthermore, we found that only the mutants  $\Delta\text{aguA1}$  and  $\Delta\text{aguA1}\Delta\text{aguA2}$  showed significantly lower survival in mice stomach than the parent strain 10403S ( $\text{Log}_{10}$  CFU: 5.7 and 5.5 versus 6.6,  $p < 0.01$ ). Complementation of *aguA1* restored its survival to a level ( $\text{Log}_{10}$  CFU: 6.5) similar to that of the parent strain (Fig. 3C). These findings suggest that only AguA1, but not AguA2, is involved in listerial resistance to acid stress, although both were induced at the mRNA level under the acidic condition.

**Expression and Purification of AguA1 and AguA2**—The two putative agmatine deiminase homologs AguA1 and AguA2 from *L. monocytogenes* were expressed in *E. coli* Rosetta (DE3) with apparent bands at expected molecular masses (46.8 kDa for AguA1 and 47.9 kDa for AguA2). His-tagged AguA1 and AguA2 were purified to homogeneity by nickel-chelated affinity column chromatography, yielding pure proteins (~20 and ~40 mg/liter culture for AguA1 and AguA2, respectively) seen as single bands on the SDS-PAGE gel (Fig. 4A).

**Optimal Conditions for Enzyme Activity**—Enzymatic activities were tested by incubation of 2.5  $\mu\text{M}$  of each enzyme in the reaction mixtures containing 10 mM agmatine or arginine as a substrate, and the product *N*-carbamoylputrescine or citrulline was measured at the indicated time points. AguA1 produced increasing amounts of *N*-carbamoylputrescine that was linear until 20 min and reached the highest level after 30 min of incubation (Fig. 4B). Specific activity was 2050 units/mg when cal-

# L. monocytogenes Agmatine Deiminase in Acid Tolerance





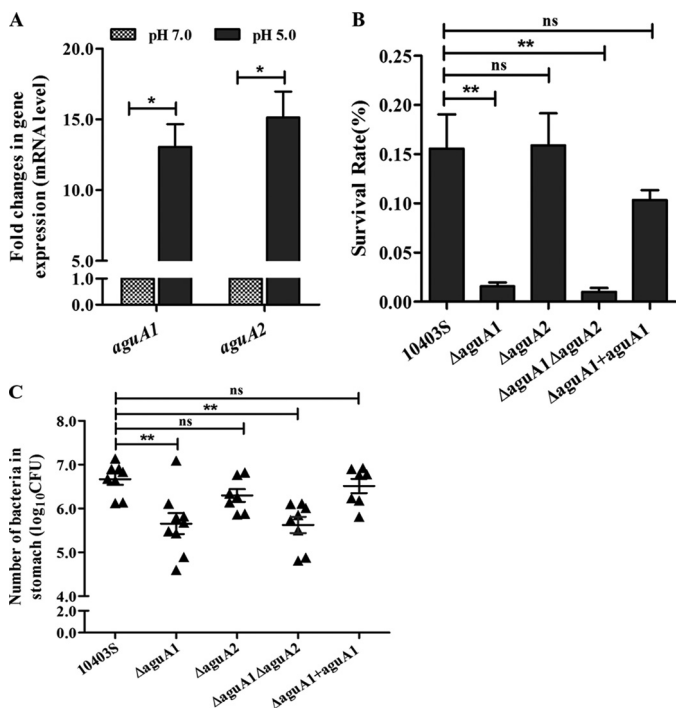


**FIGURE 3. Responses or roles of *aguA1* and *aguA2* under acidic stresses.** *A*, relative quantification of *aguA1* and *aguA2* mRNA levels in *L. monocytogenes* 10403S exposed to BHI medium at pH 5.0 and 7.0. Values are expressed as means  $\pm$  S.D. *B*, survival of *L. monocytogenes* 10403S, its mutant, and complement strains in synthetic human gastric fluid at pH 2.5. Values are expressed as means  $\pm$  S.D. *C*, survival of *L. monocytogenes* 10403S, its mutant, and complement strains in the stomach of mice receiving intragastric inoculation. Values are expressed as means  $\pm$  S.E. \*,  $p < 0.05$ ; \*\*,  $p < 0.01$ ; ns,  $p > 0.05$ .

culated from the linear range in the presence of agmatine. No citrulline was formed when arginine was used as the substrate for AguA1. However, AguA2 showed no deiminase activity either on agmatine (Fig. 4B) or on arginine (data not shown) as the substrate, suggesting that only AguA1, but not AguA2, acts as the functional agmatine deiminase in *L. monocytogenes*.

AguA1 exhibited high agmatine deiminase activity in a wide range of pH conditions from 3.5 to 10.5 with optimal pH at 7.5 (Fig. 4C), suggesting that the activity of AguA1 is not sensitive to pH, which is consistent with its contribution to acid tolerance under low pH conditions (Fig. 3, B and C). However, AguA1 showed varying activities at different temperatures, optimal at 25 °C and the residual activity was 39 and 12% at 37 and 45 °C, respectively (Fig. 4D).

**Kinetic Properties of AguA1**—AguA1 was tested for its kinetic properties under the optimal conditions at 25 °C and pH 7.5 by incubating 2.5  $\mu$ M of the enzyme in the reaction mixtures containing 10 mM agmatine as the substrate. Plotting of enzymatic velocity against substrate concentrations yielded a curve that fits the classical Michaelis-Menten model:  $K_m$ ,  $V_{max}$ ,  $k_{cat}$ , and  $k_{cat}/K_m$  values of the enzyme were  $0.65 \pm 0.23$  mM,  $85.69 \pm 7.58$   $\mu$ M/min,  $34.28 \pm 3.03$  min<sup>-1</sup>, and  $5.30 \times 10^4$  min<sup>-1</sup> M<sup>-1</sup>, respectively (Table 1 and Fig. 4E). The  $K_m$  value of AguA1 is

similar to that for *P. aeruginosa* AgDI (0.6 mM) (37) but much higher than those for maize shoots (12  $\mu$ M) (38), cucumber (16  $\mu$ M) (39), *Arabidopsis thaliana* (112  $\mu$ M) (40), *E. faecalis* (35  $\mu$ M) (5), and *Helicobacter pylori* (33  $\mu$ M) (30). However, the  $k_{cat}/K_m$  value we obtained was quite close to that of *P. aeruginosa* AgDI ( $4.2 \times 10^5$  min<sup>-1</sup> M<sup>-1</sup>) (37), *H. pylori* AgDI ( $1.47 \times 10^5$  min<sup>-1</sup> M<sup>-1</sup>) (30), and peptidyl-arginine deiminase 4 ( $3.0 \times 10^5$  min<sup>-1</sup> M<sup>-1</sup>) (31), indicating that AguA1 is a functional AgDI enzyme with reasonable kinetic properties.

**Substrate Specificity and Competitive Assay of AguA1**—Agmatine has been identified as the sole and preferred substrate for AgDIs of soybean (41), *H. pylori* (30), *P. aeruginosa* (37), *E. faecalis* (5), and *L. brevis* (8). A variety of guanidinium-containing small molecules (agmatine analogs) fail to substitute for agmatine as substrates for this enzyme. To determine whether AguA1 also has similar substrate specificity, L-arginine, another guanidinium-containing compound, was used to see whether it could be utilized by AguA1. Fig. 4F shows that there was no formation of citrulline from L-arginine in the presence of AguA1, indicating that L-arginine does not act as the substrate for AguA1. Moreover, arginine showed no competitive effect on agmatine even at high concentrations up to 10 mM (Fig. 4F). Thus, AguA1 demonstrates distinct preference for agmatine, as is the case with other AgDIs.

**Metal Inhibition of AguA1**—Metal ions Cu<sup>2+</sup>, Zn<sup>2+</sup>, and Co<sup>2+</sup> inhibited AguA1 with varying degrees of potency with respective IC<sub>50</sub> of  $0.034 \pm 0.008$  mM (Fig. 5A),  $0.25 \pm 0.05$  mM (Fig. 5B), and  $2.89 \pm 0.82$  mM (Fig. 5C), indicating that copper ion is the most inhibitory. There was no inhibitory effect on AguA1 activity with Fe<sup>3+</sup>, Mg<sup>2+</sup>, and Ni<sup>2+</sup> ions, even at highest concentrations (10 mM) (data not shown). These results suggest that the active sites of AguA1 could be susceptible to such metal ions as Cu<sup>2+</sup>, Zn<sup>2+</sup>, and Co<sup>2+</sup>.

**Thermostability of AguA1**—The purified enzyme preparation, when stored at 4 °C, maintained activity for at least 1 month (85% activity retained). However, 80% of the activity was lost when it was exposed to 25 °C for 6 h (Fig. 5D), indicating that AguA1 is sensitive to temperature, and its purification should proceed under 4 °C.

**Effect of Site-directed Mutagenesis on the Activities of AguA1 and AguA2**—Bioinformatic analysis suggests that Asp-94, Glu-155, His-216, Asp-218, and Cys-356 could be the corresponding catalytic residues for AguA1 and AguA2 (Fig. 2B). These residues were substituted by site-directed mutagenesis. The mutant proteins were expressed and purified, and their enzymatic activity was characterized in a way identical to that of the wild-type enzyme. Mutant proteins at D94A, E155A, H216A, D218A, and C356A completely lost their ability to degrade agmatine (Fig. 6A). Mutants substituted with amino acids of similar biochemical properties at the same sites (D94E, E155D, H216R, and D218E) also lost the enzyme activity (Fig. 6A). Therefore, kinetic analysis was not applied to these mutant pro-

**FIGURE 2. Bioinformatic analysis of AguA1 and AguA2.** *A*, phylogenetic tree of AguA1/AguA2 and homologs from other bacterial species. The tree was constructed by the neighbor-joining program, and a bootstrap test of 100 replicates was used to estimate the confidence of branching patterns, where the numbers on internal nodes are the support values. *B*, amino acid sequence alignment of AguA1/AguA2 against homologs from *A. thaliana*, *H. pylori*, *S. mutans*, *E. faecalis*, *L. lactis*, and *P. aeruginosa*. The conserved motifs and residues are shaded. The key amino acid residues noted with asterisks are involved in substrate binding and enzyme activity. The boxed residues are different between AguA2 and AguA1 or other AgDIs.

## *L. monocytogenes* Agmatine Deiminase in Acid Tolerance

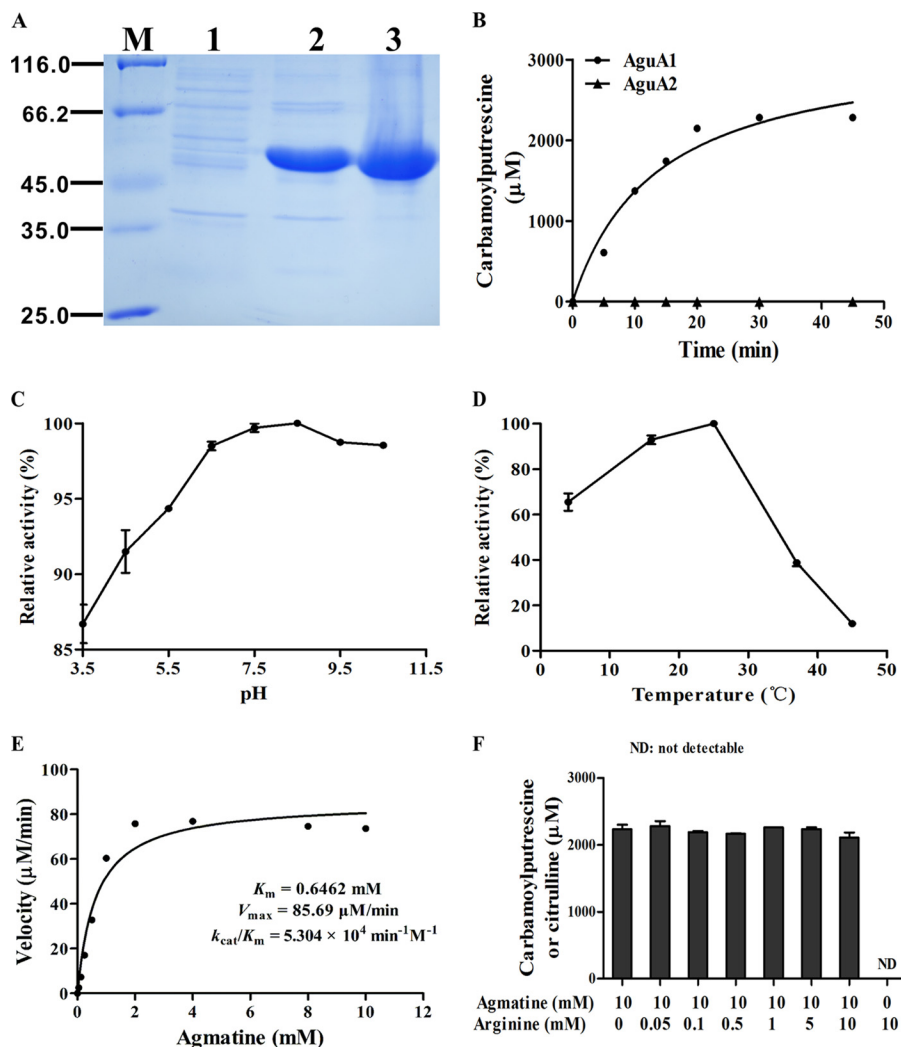


**FIGURE 4. Gel electrophoresis of AguA1 and AguA2 expressed in *E. coli* and enzymatic characterization of AguA1.** A, SDS-PAGE analysis of the recombinant AguA1 and AguA2 proteins. Lane M, molecular mass standards; lane 1, supernatant of *E. coli* harboring pET30a; lanes 2 and 3, purification of AguA1 and AguA2, respectively. B, time course analysis of AguA1 and AguA2 activity with 10 mM agmatine. C, effect of pH on AguA1 activity. D, effect of temperature on AguA1 activity. E, Michaelis-Menten plot of AguA1 determined by measuring the enzymatic velocity. F, substrate specificity and competitive assay of AguA1 in the presence of 10 mM of agmatine and varying concentration (0–10 mM) of arginine. ND, not detectable.

**TABLE 1**  
Steady-state kinetic constants measured for agmatine with wild-type and mutant AguA1 enzymes

Enzyme	$V_{max}$ $\mu\text{M}/\text{min}$	$k_{cat}$ $\text{min}^{-1}$	$K_m$ $\text{mM}$	$k_{cat}/K_m$ $\text{min}^{-1} \text{ M}^{-1}$
Wild-type	$85.69 \pm 7.58$	$34.28 \pm 3.03$	$0.65 \pm 0.23$	$5.30 \times 10^4$
D94A			Inactive	
E155A			Inactive	
H216A			Inactive	
D218A			Inactive	
C356A			Inactive	
D94E			Inactive	
E155D			Inactive	
H216R			Inactive	
D218E			Inactive	
G157C			Inactive	

teins (Table 1). These results indicate that the corresponding residues in *L. monocytogenes* AguA1 play a critical and irreplaceable role in its catalytic activity, consistent with those obtained for other AgDIs and ADIs (30, 34, 42, 43).

AguA2 did not show any deiminase activity (Fig. 4B), although it has high homology and similar crystal model

to AguA1, including the five critical residues (Fig. 2B and supplemental Fig. S1). However, we found that there are five specific residues (Tyr-47, Cys-157, Phe-196, Asn-236, and His-360) of AguA2 that differ from AguA1 and other AgDIs (corresponding residues: Phe, Gly, Leu, Asp, and Gln) (Fig. 2B), which might account for the loss of its deiminase activity. To verify our hypothesis, site-directed mutant proteins at Y47F, C157G, F196L, N236D, and H360Q for AguA2 were generated, and their enzymatic activity was determined. Interestingly, we found that AguA2 acquired agmatine deiminase activity only when Cys-157 was mutated to Gly, whereas the other mutants were still inactive (Fig. 6B). We also confirmed that AguA1 with G157C mutation led to the complete loss of the enzyme activity (Fig. 6C). This is the first time that Gly-157 has been discovered as a key residue in addition to those known to be essential for AgDI activity. Protein BLAST did not show any mutation with Gly-157 from the available UniProt Protein database for *L. monocytogenes*, further confirming that AguA1 is the only functional AgDI in this bacterium.

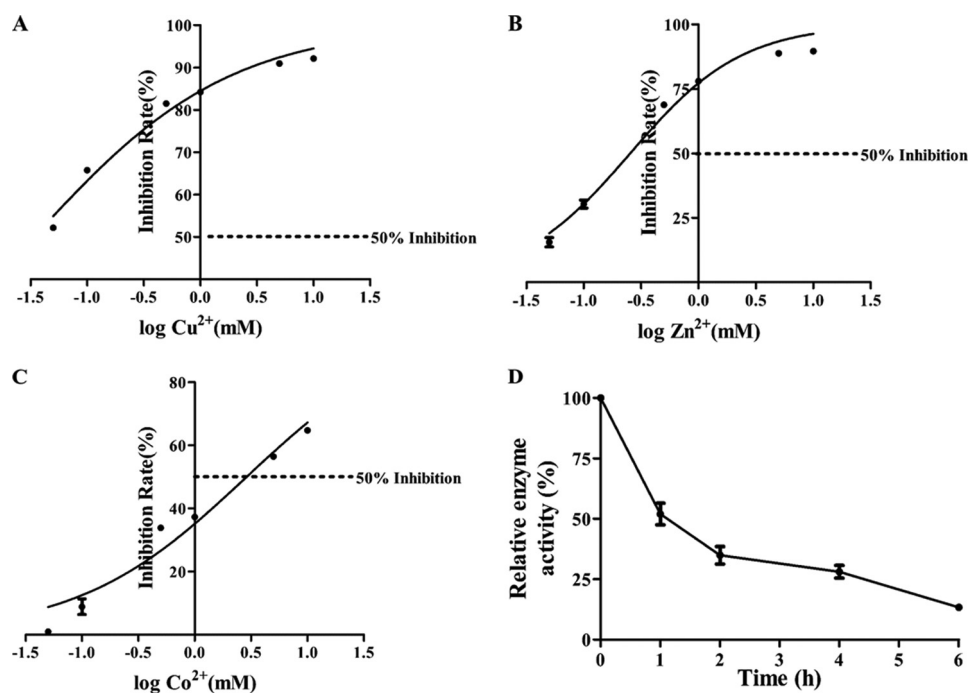


FIGURE 5. **Enzymatic stability of AguA1 in the presence of metal ions and at room temperature.** A–C, effects of metal ions Cu<sup>2+</sup> (A), Zn<sup>2+</sup> (B), and Co<sup>2+</sup> (C) up to 10 mM on AguA1 activity. The dotted lines represent 50% inhibition of the enzyme activity (I<sub>C50</sub>). D, effect of room temperature at 25 °C on stability of AguA1.

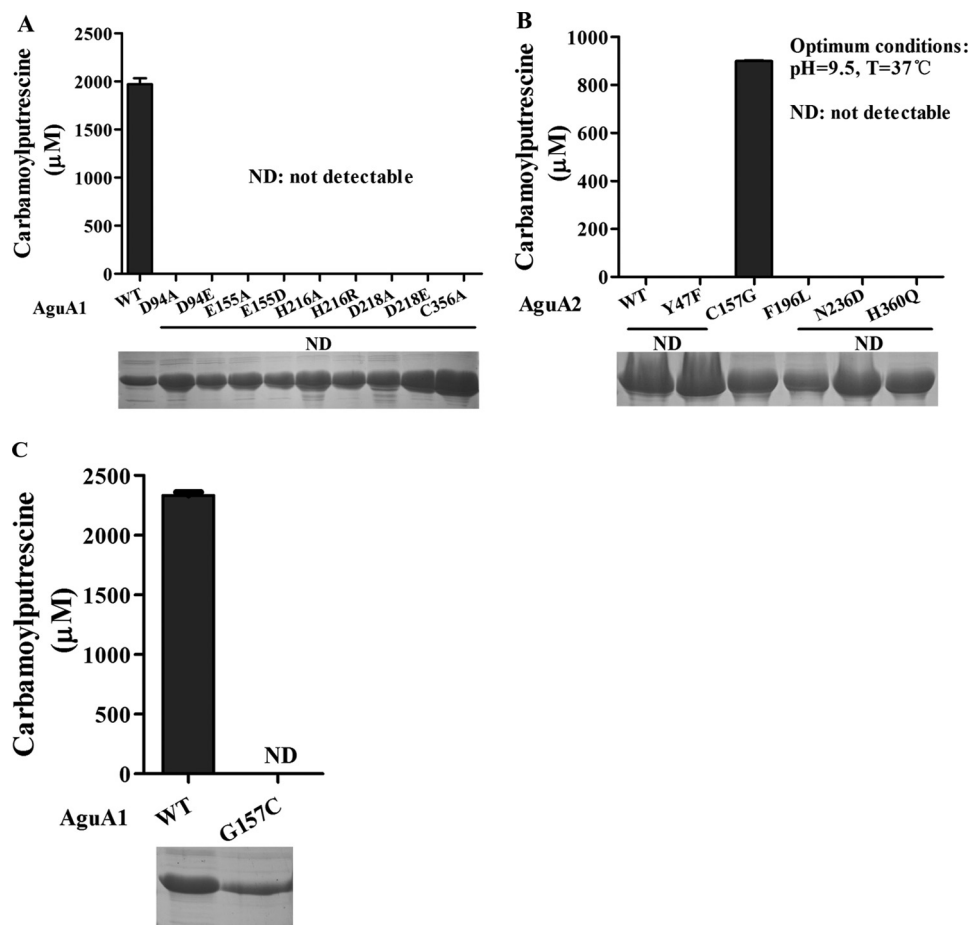


FIGURE 6. **Enzymatic activity of wild-type AguA1 and AguA2 and their mutant proteins.** A, relative activity of wild-type AguA1 and its mutants (D94A/D94E, E155A/E155D, H216A/H216R, D218A/D218E, and C356A). B, enzymatic activity of wild-type AguA2 and its mutants (Y47F, C157G, F196L, N236D, and H360Q). C, enzymatic activity of wild-type AguA1 and its mutant G157C. ND, not detectable.



### DISCUSSION

The ability of *Listeria monocytogenes* to tolerate low pH environments is of importance to its pathogenicity because the pathogen encounters acidic environments in the nature and food processing industry *in vitro* and during passage through the stomach or even within macrophage phagosomes *in vivo* (44). A number of acid resistance mechanisms have been identified in *L. monocytogenes*, such as glutamate decarboxylase and ADI systems, and F<sub>1</sub>F<sub>0</sub>-ATPase (2, 37, 45). The AgDI pathway generally contains a panel of genes coding for AgDI, putrescine transcarbamoylase, carbamate kinase, and agmatine-putrescine exchanger (8). However, there are two putative AgDI homologs, AguA1 and AguA2, encoded by *aguA1* and *aguA2*, respectively, in *L. monocytogenes*. This is also seen in *L. brevis* IOEB 9809, *Lactobacillus sakei*, and *Pediococcus pentosaceus* (8). AgDI is one of the three crucial enzymes constituting the AgDI pathway, which deiminates the substrate agmatine to produce *N*-carbamoylputrescine and NH<sub>3</sub>. Ammonia can combine with intracellular cytoplasmic protons to yield ammonium ions (NH<sub>4</sub><sup>+</sup>), thereby alleviating acidification of the cytoplasm and contributing to pH homeostasis (6, 7, 46).

Initially, we found that both *aguA1* and *aguA2* were induced at the mRNA level when *L. monocytogenes* was subjected to low pH at 5.0, suggesting that both AguA1 and AguA2 could be involved in acid tolerance (Fig. 3A). However, only the  $\Delta$ *aguA1* mutant, but not the  $\Delta$ *aguA2* mutant, exhibited significant reduction of its survival both in synthetic human gastric fluid (pH 2.5) and mice stomach, as compared with its parent and complemented strains (Fig. 3, B and C). Enzyme assays revealed that *L. monocytogenes* AguA1 had typical substrate specificity of AgDI, whereas AguA2 showed no deiminase activity. However, we found a specific residue, Cys-157, of AguA2 differing from other AgDIs including AguA1 that could be involved in AgDI activity because the mutant AguA2 at C157G converted agmatine to *N*-carbamoylputrescine. To our surprise, single mutation of G157C of AguA1 led to the loss of its enzyme activity. Further bioinformatic search reveals that Gly-157 for AguA1 and Cys-157 for AguA2 are conserved in all *L. monocytogenes* sequences (total 68 sequences) available in UniProt protein database. Therefore, we come to the conclusion that AguA1 is the only functional AgDI that contributes to acid tolerance of *L. monocytogenes*. To our knowledge, This is the first time that Gly-157 has been uncovered as another key residue other than those previously found essential for AgDI activity.

The AgDI pathway closely resembles the ADI pathway. The two pathways consist of similar enzymes performing similar reactions but only differ in their substrates. ADI catalyzes deimination of L-arginine but not L-agmatine, whereas AgDI catalyzes deimination of agmatine but not L-arginine. Although ADI and AgDI are structurally divergent in the region of the active site that interacts with the C<sup>α</sup>H(NH<sub>3</sub><sup>+</sup>)(COO<sup>-</sup>) region of the substrate, the regions that interact with the guanidino group of the substrate are quite similar (43). Despite their unique substrate specificity, both ADIs and AgDIs contain a highly conserved catalytic triad (Cys-His-Glu/Asp). In this study, site-directed mutagenesis indicates that Asp-94, Glu-155, His-216, Asp-218, and Cys-356 are the corresponding cat-

alytic residues in *L. monocytogenes* AguA1 because single mutation at any one of these residues completely abolished the enzymatic activity (Table 1 and Fig. 6). Although these residues are also present in AguA2, there was no enzyme activity unless the Cys-157 residue was mutated to glycine as discussed above. Our findings expand the current understanding of microbial AgDIs including *L. monocytogenes* with a novel key residue uncovered as having catalytic activity (30, 34, 42, 43). The AguA1 of *L. monocytogenes* most likely employs similar catalytic mechanisms of the guanidinium-modifying enzyme family previously described (30, 34, 35).

In conclusion, *L. monocytogenes* harbors two putative agmatine deiminases, but only AguA1 functionally participates in the AgDI pathway and contributes to its acid tolerance. AguA1 is specific for agmatine catalysis, sensitive to some metal ions such as Cu<sup>2+</sup>, Zn<sup>2+</sup>, and Co<sup>2+</sup>, and optimal at 25 °C and over a wide range of pH from 3.5 to 10.5. We have also discovered a novel residue Gly-157 other than the known catalytic triad (Cys-His-Glu/Asp) critical for *L. monocytogenes* AgDI activity. Further research is required to examine the role of *aguD*, as the agmatine-putrescine antiporter, in the proposed AgDI system of *L. monocytogenes* and in acid tolerance.

---

*Acknowledgment*—We thank Dr. Martin Wiedmann at Cornell University for kindly providing the shuttle plasmid pKSV7.

---

### REFERENCES

- Vázquez-Boland, J. A., Kuhn, M., Berche, P., Chakraborty, T., Domínguez-Bernal, G., Goebel, W., González-Zorn, B., Wehland, J., and Kreft, J. (2001) *Listeria pathogenesis* and molecular virulence determinants. *Clin. Microbiol. Rev.* **14**, 584–640
- Corr, S. C., and O'Neill, L. A. (2009) *Listeria monocytogenes* infection in the face of innate immunity. *Cell Microbiol.* **11**, 703–709
- Cotter, P. D., and Hill, C. (2003) Surviving the acid test. Responses of gram-positive bacteria to low pH. *Microbiol. Mol. Biol. Rev.* **67**, 429–453
- Gray, M. J., Freitag, N. E., and Boor, K. J. (2006) How the bacterial pathogen *Listeria monocytogenes* mediates the switch from environmental Dr. Jekyll to pathogenic Mr. Hyde. *Infect. Immun.* **74**, 2505–2512
- Llácer, J. L., Polo, L. M., Tavárez, S., Alarcón, B., Hilario, R., and Rubio, V. (2007) The gene cluster for agmatine catabolism of *Enterococcus faecalis*. Study of recombinant putrescine transcarbamylase and agmatine deiminase and a snapshot of agmatine deiminase catalyzing its reaction. *J. Bacteriol.* **189**, 1254–1265
- Griswold, A. R., Jameson-Lee, M., and Burne, R. A. (2006) Regulation and physiologic significance of the agmatine deiminase system of *Streptococcus mutans* UA159. *J. Bacteriol.* **188**, 834–841
- Griswold, A. R., Chen, Y. Y., and Burne, R. A. (2004) Analysis of an agmatine deiminase gene cluster in *Streptococcus mutans* UA159. *J. Bacteriol.* **186**, 1902–1904
- Lucas, P. M., Blancato, V. S., Claisse, O., Magni, C., Lolkema, J. S., and Lonvaud-Funel, A. (2007) Agmatine deiminase pathway genes in *Lactobacillus brevis* are linked to the tyrosine decarboxylation operon in a putative acid resistance locus. *Microbiology* **153**, 2221–2230
- Driessen, A. J., Smid, E. J., and Konings, W. N. (1988) Transport of diamines by *Enterococcus faecalis* is mediated by an agmatine-putrescine antiporter. *J. Bacteriol.* **170**, 4522–4527
- Chen, J., Cheng, C., Xia, Y., Zhao, H., Fang, C., Shan, Y., Wu, B., and Fang, W. (2011) Lmo0036, an ornithine and putrescine carbamoyltransferase in *Listeria monocytogenes*, participates in arginine deiminase and agmatine deiminase pathways and mediates acid tolerance. *Microbiology* **157**, 3150–3161
- Liu, Y., Zeng, L., and Burne, R. A. (2009) *AguR* is required for induction of

- the *Streptococcus mutans* agmatine deiminase system by low pH and agmatine. *Appl. Environ. Microbiol.* **75**, 2629–2637
12. Shirai, H., Blundell, T. L., and Mizuguchi, K. (2001) A novel superfamily of enzymes that catalyze the modification of guanidino groups. *Trends Biochem. Sci.* **26**, 465–468
  13. Shirai, H., Mokrab, Y., and Mizuguchi, K. (2006) The guanidino-group modifying enzymes. Structural basis for their diversity and commonality. *Proteins* **64**, 1010–1023
  14. Glaser, P., Frangeul, L., Buchrieser, C., Rusniok, C., Amend, A., Baquero, F., Berche, P., Bloecker, H., Brandt, P., Chakraborty, T., Charbit, A., Chetouani, F., Couvé, E., de Daruvar, A., Dehoux, P., Domann, E., Domínguez-Bernal, G., Duchaud, E., Durant, L., Dussurget, O., Entian, K. D., Fsihi, H., García-del Portillo, F., Garrido, P., Gautier, L., Goebel, W., Gómez-López, N., Hain, T., Haut, J., Jackson, D., Jones, L. M., Kaerst, U., Kreft, J., Kuhn, M., Kunst, F., Kurapkat, G., Madueno, E., Maitournam, A., Vicente, J. M., Ng, E., Nedjari, H., Nordsiek, G., Novella, S., de Pablos, B., Pérez-Díaz, J. C., Purcell, R., Rimmel, B., Rose, M., Schlueter, T., Simoes, N., Tierrez, A., Vazquez-Boland, J. A., Voss, H., Wehland, J., and Cossart, P. (2001) Comparative genomics of *Listeria* species. *Science* **294**, 849–852
  15. Chen, J., Jiang, L., Chen, Q., Zhao, H., Luo, X., Chen, X., and Fang, W. (2009) lmo0038 is involved in acid and heat stress responses and specific for *Listeria monocytogenes* lineages I and II, and *Listeria ivanovii*. *Foodborne Pathog. Dis.* **6**, 365–376
  16. Cotter, P. D., Gahan, C. G., and Hill, C. (2001) A glutamate decarboxylase system protects *Listeria monocytogenes* in gastric fluid. *Mol. Microbiol.* **40**, 465–475
  17. Cotter, P. D., O'Reilly, K., and Hill, C. (2001) Role of the glutamate decarboxylase acid resistance system in the survival of *Listeria monocytogenes* LO28 in low pH foods. *J. Food Prot.* **64**, 1362–1368
  18. Ryan, S., Begley, M., Gahan, C. G., and Hill, C. (2009) Molecular characterization of the arginine deiminase system in *Listeria monocytogenes*. Regulation and role in acid tolerance. *Environ. Microbiol.* **11**, 432–445
  19. Cheng, C., Chen, J., Shan, Y., Fang, C., Liu, Y., Xia, Y., Song, H., and Fang, W. (2013) *Listeria monocytogenes* ArcA contributes to acid tolerance. *J. Med. Microbiol.* **62**, 813–821
  20. Wiedmann, M., Arvik, T. J., Hurley, R. J., and Boor, K. J. (1998) General stress transcription factor sigmaB and its role in acid tolerance and virulence of *Listeria monocytogenes*. *J. Bacteriol.* **180**, 3650–3656
  21. Arnold, K., Bordoli, L., Kopp, J., and Schwede, T. (2006) The SWISS-MODEL workspace. A web-based environment for protein structure homology modelling. *Bioinformatics* **22**, 195–201
  22. Bordoli, L., Kiefer, F., Arnold, K., Benkert, P., Battey, J., and Schwede, T. (2009) Protein structure homology modeling using SWISS-MODEL workspace. *Nat. Protoc.* **4**, 1–13
  23. Bordoli, L., and Schwede, T. (2012) Automated protein structure modeling with SWISS-MODEL workspace and the protein model portal. *Methods Mol. Biol.* **857**, 107–136
  24. Livak, K. J., and Schmittgen, T. D. (2001) Analysis of relative gene expression data using real-time quantitative PCR and the  $2(-\Delta\Delta C(T))$  method. *Methods* **25**, 402–408
  25. Chen, J., Jiang, L., Chen, X., Luo, X., Chen, Y., Yu, Y., Tian, G., Liu, D., and Fang, W. (2009) *Listeria monocytogenes* serovar 4a is a possible evolutionary intermediate between *L. monocytogenes* serovars 1/2a and 4b and *L. innocua*. *J. Microbiol. Biotechnol.* **19**, 238–249
  26. Jiang, L., Chen, J., Xu, J., Zhang, X., Wang, S., Zhao, H., Vongxay, K., and Fang, W. (2008) Virulence characterization and genotypic analyses of *Listeria monocytogenes* isolates from food and processing environments in eastern China. *Int. J. Food Microbiol.* **121**, 53–59
  27. Monk, I. R., Gahan, C. G., and Hill, C. (2008) Tools for functional post-genomic analysis of *Listeria monocytogenes*. *Appl. Environ. Microbiol.* **74**, 3921–3934
  28. Camilli, A., Tilney, L. G., and Portnoy, D. A. (1993) Dual roles of plcA in *Listeria monocytogenes* pathogenesis. *Mol. Microbiol.* **8**, 143–157
  29. van Netten, P., Perales, I., van de Moosdijk, A., Curtis, G. D., and Mossel, D. A. (1989) Liquid and solid selective differential media for the detection and enumeration of *L. monocytogenes* and other *Listeria* spp. *Int. J. Food Microbiol.* **8**, 299–316
  30. Jones, J. E., Causey, C. P., Lovelace, L., Knuckley, B., Flick, H., Lebioda, L., and Thompson, P. R. (2010) Characterization and inactivation of an agmatine deiminase from *Helicobacter pylori*. *Bioorg. Chem.* **38**, 62–73
  31. Kearney, P. L., Bhatia, M., Jones, N. G., Yuan, L., Glascock, M. C., Catchings, K. L., Yamada, M., and Thompson, P. R. (2005) Kinetic characterization of protein arginine deiminase 4. A transcriptional corepressor implicated in the onset and progression of rheumatoid arthritis. *Biochemistry* **44**, 10570–10582
  32. Knipp, M., and Vasák, M. (2000) A colorimetric 96-well microtiter plate assay for the determination of enzymatically formed citrulline. *Anal. Biochem.* **286**, 257–264
  33. Jones, J. E., Dreyton, C. J., Flick, H., Causey, C. P., and Thompson, P. R. (2010) Mechanistic studies of agmatine deiminase from multiple bacterial species. *Biochemistry* **49**, 9413–9423
  34. Galkin, A., Lu, X., Dunaway-Mariano, D., and Herzberg, O. (2005) Crystal structures representing the Michaelis complex and the thiuronium reaction intermediate of *Pseudomonas aeruginosa* arginine deiminase. *J. Biol. Chem.* **280**, 34080–34087
  35. Das, K., Butler, G. H., Kwiatkowski, V., Clark, A. D., Jr., Yadav, P., and Arnold, E. (2004) Crystal structures of arginine deiminase with covalent reaction intermediates. Implications for catalytic mechanism. *Structure* **12**, 657–667
  36. Galkin, A., Kulakova, L., Sarikaya, E., Lim, K., Howard, A., and Herzberg, O. (2004) Structural insight into arginine degradation by arginine deiminase, an antibacterial and parasite drug target. *J. Biol. Chem.* **279**, 14001–14008
  37. Nakada, Y., and Itoh, Y. (2003) Identification of the putrescine biosynthetic genes in *Pseudomonas aeruginosa* and characterization of agmatine deiminase and *N*-carbamoylputrescine amidohydrolase of the arginine decarboxylase pathway. *Microbiology* **149**, 707–714
  38. Yanagisawa, H. (2001) Agmatine deiminase from maize shoots. Purification and properties. *Phytochemistry* **56**, 643–647
  39. Sakakibara, Y., and Yanagisawa, H. (2003) Agmatine deiminase from cucumber seedlings is a mono-specific enzyme. Purification and characteristics. *Protein Expr. Purif.* **30**, 88–93
  40. Janowitz, T., Kneifel, H., and Piotrowski, M. (2003) Identification and characterization of plant agmatine iminohydrolase, the last missing link in polyamine biosynthesis of plants. *FEBS Lett.* **544**, 258–261
  41. Park, K. H., and Cho, Y. D. (1991) Purification of monomeric agmatine iminohydrolase from soybean. *Biochem. Biophys. Res. Commun.* **174**, 32–36
  42. Wei, Y., Zhou, H., Sun, Y., He, Y., and Luo, Y. (2007) Insight into the catalytic mechanism of arginine deiminase. Functional studies on the crucial sites. *Proteins* **66**, 740–750
  43. Lu, X., Li, L., Wu, R., Feng, X., Li, Z., Yang, H., Wang, C., Guo, H., Galkin, A., Herzberg, O., Mariano, P. S., Martin, B. M., and Dunaway-Mariano, D. (2006) Kinetic analysis of *Pseudomonas aeruginosa* arginine deiminase mutants and alternate substrates provides insight into structural determinants of function. *Biochemistry* **45**, 1162–1172
  44. O'Driscoll, B., Gahan, C. G., and Hill, C. (1996) Adaptive acid tolerance response in *Listeria monocytogenes*. Isolation of an acid-tolerant mutant which demonstrates increased virulence. *Appl. Environ. Microbiol.* **62**, 1693–1698
  45. Cotter, P. D., Gahan, C. G., and Hill, C. (2000) Analysis of the role of the *Listeria monocytogenes* FOF1-ATPase operon in the acid tolerance response. *Int. J. Food Microbiol.* **60**, 137–146
  46. Cunin, R., Glansdorff, N., Piérard, A., and Stalon, V. (1986) Biosynthesis and metabolism of arginine in bacteria. *Microbiol. Rev.* **50**, 314–352